



## Open Archive Toulouse Archive Ouverte

OATAO is an open access repository that collects the work of Toulouse researchers and makes it freely available over the web where possible

This is an author's version published in: <http://oatao.univ-toulouse.fr/20612>

**Official URL:**

<http://dx.doi.org/10.1103/PhysRevE.77.026310>

**To cite this version:**

Elhajjar, Bilal and Charrier-Mojtabi, Marie-Catherine and Mojtabi, Abdelkader *Separation of a binary fluid mixture in a porous horizontal cavity* (2008) Fluid Dynamics Research, 77, n°2. pp. 1 - 6. ISSN 1539-3755

Any correspondence concerning this service should be sent to the repository administrator: [tech-oatao@listes-diff.inp-toulouse.fr](mailto:tech-oatao@listes-diff.inp-toulouse.fr)

# Separation of a binary fluid mixture in a porous horizontal cavity

Bilal Elhajjar,<sup>1</sup> Marie-Catherine Charrier-Mojtabi,<sup>2,\*</sup> and Abdelkader Mojtabi<sup>1</sup>

<sup>1</sup>IMFT, UMR CNRS/INP/UPS No 5502, UFR MIG, Université Paul Sabatier, 118 Route de Narbonne, 31062, Toulouse Cedex, France

<sup>2</sup>Laboratoire PHASE, EA 3028, UFR PCA, Université Paul Sabatier, 118 Route de Narbonne, 31062, Toulouse Cedex, France

Thermogravitational separation has, until now, been used in differentially heated vertical cells, called thermogravitational columns (TGCs). The cell can be either a slit or an annular cavity whose two isothermal faces are maintained at different temperatures  $T_1$  and  $T_2$ . In this study, we show contrary to what has been done until now, that it is possible to carry out the separation of the species of a binary mixture in the classical configuration of Rayleigh-Bénard (horizontal cell heated from below with the separation ratio  $\psi > \psi_{\text{mono}} > 0$  or from above with  $\psi < 0$ ); we obtain a monocellular flow for  $\psi > \psi_{\text{mono}}$  at the onset of convection. The species separation, in a horizontal cell, is obtained without fear of the remixing observed in vertical thermogravitational cells for fluids with negative Soret coefficients. In this situation, the heaviest component concentrates in the upper part of the cell creating an unstable physical situation. We improve the efficiency of separation for the development of an industrial process of separation. We study the thermogravitational separation of the components of a binary fluid mixture saturating a horizontal porous layer, in the presence of the Soret effect. The horizontal walls of the cavity are impermeable and maintained at constant and different temperatures. The system of equations governing the problem has an equilibrium solution with a vertical stratification of temperature and concentration. This solution loses its stability via a stationary bifurcation for values of the separation ratio  $\psi > \psi_0$  while, for  $\psi < \psi_0$ , stability is lost via a Hopf bifurcation. For a cavity heated from below, the flow resulting from the stationary bifurcation becomes monocellular beyond a certain value of  $\psi > \psi_{\text{mono}} > 0$  and leads to a separation of the species between the two ends of the cell. We propose to determine whether the monocellular flow remains stable until the optimum of separation and if we can obtain high separation in the case of a horizontal cavity. We verify that the critical Rayleigh number  $\text{Ra}_{c_2}$ , associated with the transition between monocellular flow and multicellular flow, is higher than the optimum Rayleigh number leading to maximum separation of species. Thus this study reveals that it is possible to obtain optimal separation before the monocellular flow loses its stability. We show also that the separation inside the horizontal cell in a Rayleigh-Bénard configuration permits us to produce the same degree of separation but with a greater quantity of each species compared to a thermogravitational vertical column.

PACS number(s): 44.25.+f, 44.30.+v, 47.20.-k, 47.90.+a

## I. INTRODUCTION

In binary fluid mixtures subjected to temperature gradients, the thermodiffusion effect induces a mass fraction gradient. In the expression of the mass flux  $\mathbf{J}$  of one of the components, in addition to the usual isothermal contribution given by the Fick law, there is an additional contribution proportional to the temperature gradient

$$\mathbf{J} = -\rho D \nabla C - \rho C(1-C) D_T \nabla T, \quad (1)$$

where  $D$  is the coefficient of mass diffusion,  $D_T$  the coefficient of thermodiffusion,  $\rho$  the density, and  $C$  the mass fraction of the denser component.

Thermogravitational diffusion is the combination of two phenomena: convection and thermal diffusion. The coupling of these two phenomena leads to species separation.

In 1938, Clusius and Dickel [1] successfully carried out the separation of gas mixtures in a vertical cavity (TGC). The following year, two fundamental theoretical and experimental works on the separation of the components of a binary mixture by thermogravitation were published. Furry, Jones, and Onsager [2] (FJO) developed the theory of ther-

modiffusion to interpret the experimental processes of separation of isotopes.

Subsequently, many works appeared, aimed at justifying the assumptions or extending the results of the theory of FJO to the case of binary liquids [3]. Other works were related to the improvement of the experimental device to increase separation. Lorenz and Emery [4] proposed the introduction of a porous medium into the cavity. Platten *et al.* [5] inclined the cavity at a certain angle to the vertical to increase separation. More recently, many works have appeared on separation using the Soret effect in binary mixtures (e.g., Labrosse [6]) or in multicomponent fluids (e.g., Ryzhkov *et al.* [7]). Bou-Ali *et al.* [8,9] were interested in mixtures with negative Soret coefficient. In all these studies, separation is analyzed in vertical thermogravitational columns. Elhajjar *et al.* [10], on the other hand, used a horizontal cavity with temperature gradients imposed on the horizontal walls to obtain two control parameters making it possible to better control the separation.

In this paper, we revisit the studies developed by many authors on the extension of the problem of Rayleigh-Bénard to binary mixtures, taking the Soret effect into account. Knobloch [11] and Platten *et al.* [12] obtained the stability diagram in which the critical Rayleigh number is given as a function of the separation ratio  $\psi$ , for a given Lewis number  $Le$ . It results from these studies in the case of a cell heated

\*cmojtabi@cict.fr

from below and for  $\psi > 0$ , that the solution of double pure diffusion loses its stability for a Rayleigh number lower than the well known value  $Ra_c = 1707.8$  obtained for the classical Rayleigh-Bénard problem. The analog study was also performed in porous media by Sovran *et al.* [13]. In all these studies in which the monocellular flow was found, no mention is made of the possibility of separation in this configuration.

In Sec. III of this paper, we present, after the mathematical formulation, an analytical solution of the monocellular flow obtained for  $\psi > \psi_{\text{mono}} > 0$  based on the hypothesis of parallel flow. Then we obtain the value of the Rayleigh number  $Ra_{\text{opt}}$  leading to the optimum separation of species associated with this convective flow. In Sec. IV, we study the stability of this monocellular flow to obtain the associated critical Rayleigh number  $Ra_{c_2}$ . We show that this critical Rayleigh number  $Ra_{c_2}$  is higher than the optimum Rayleigh number. In Sec. V, several numerical simulations are carried out in order to corroborate the theoretical results obtained for the separation of species and from the linear stability analysis. In Sec. VI, we compare the separation evolution versus  $Ra$  obtained in a classical thermogravitational column and in a Rayleigh-Bénard cell.

## II. MATHEMATICAL FORMULATION

We consider a cavity of height  $H$ , length  $L$ , and of high aspect ratio  $A = L/H$ , filled with a porous medium and saturated by a binary mixture. The flow domain is  $\Omega = [0, L] \times [0, H]$ . The horizontal walls are maintained at constant and different temperatures  $T_1$  and  $T_2$ , the vertical walls are adiabatic and all the walls are impermeable. We use the following assumptions. (i) The temperature differences are sufficiently small for the Boussinesq approximation to be used. (ii) The Dufour effect is neglected. The density variation with temperature and mass fraction is described by the state equation

$$\rho = \rho_r [1 - \beta_T(T - T_r) - \beta_C(C - C_r)], \quad (2)$$

where  $\rho_r$  is the fluid mixture density at temperature  $T_r$  and mass fraction  $C_r$ .  $\beta_T$  and  $\beta_C$  are the thermal and concentration expansion coefficients, respectively.

Using these approximations, the equations of continuity, momentum transport, energy transport and species transport, with the Soret effect in a dimensionless form can be written as

$$\begin{aligned} \nabla \cdot \mathbf{V} &= 0, \\ \nabla P + \mathbf{V} &= Ra(T + \psi C) \hat{\mathbf{e}}_z, \\ \frac{\partial T}{\partial t} + \mathbf{V} \cdot \nabla T &= \nabla^2 T, \\ \varepsilon^* \frac{\partial C}{\partial t} + \mathbf{V} \cdot \nabla C &= \frac{1}{Le} \nabla^2 (C - T). \end{aligned} \quad (3)$$

The above equations were obtained using the following dimensionless quantities:  $H$  for length,  $\lambda^*/[H(\rho c)_f]$  for veloc-

ity,  $[(\rho c)^* H^2]/\lambda^*$  for time,  $(\lambda^* \mu)/[K(\rho c)_f]$  for pressure,  $\Delta T = T_1 - T_2$  for temperature, and  $\Delta C = -\Delta T C_i (1 - C_i) (D_T^*/D^*)$  for mass fraction.

This problem depends on five dimensionless parameters: the thermal Rayleigh number  $Ra = (Kg\beta_T H \Delta T)/(a^* \nu)$ , the solutal to thermal buoyancy ratio  $\psi = -(\beta_C/\beta_T) \times (D_T^*/D^*) C_i (1 - C_i)$ , the Lewis number  $Le = a^*/D^*$ , the normalized porosity  $\varepsilon^* = \varepsilon(\rho c)_f/(\rho c)^*$ , and the aspect ratio  $A$ . Here  $\nu$  is the kinematic viscosity of the fluid mixture,  $K$  the permeability of the porous medium,  $(\rho c)^*$  the effective volumetric heat capacity,  $(\rho c)_f$  the volumetric heat capacity of fluid,  $\lambda^*$  the effective thermal conductivity,  $a^*$  the thermal diffusivity,  $\varepsilon$  the porosity,  $D^*$  and  $D_T^*$  the mass diffusive and thermal diffusive coefficients, and  $C_i$  the initial mass fraction coefficient of the denser species.

The corresponding boundary conditions are

$$T = 1 \quad \text{for } z = 0, \quad T = 0 \quad \text{for } z = 1,$$

$$\nabla C \cdot \mathbf{n} = \nabla T \cdot \mathbf{n} \quad \text{for } z = 0, 1,$$

$$\partial T / \partial x = \partial C / \partial x = 0 \quad \text{for } x = 0, A,$$

$$\mathbf{V} \cdot \mathbf{n} = 0 \quad \forall M \in \partial\Omega. \quad (4)$$

This system of equations has an equilibrium solution  $(T_0, C_0, \mathbf{V}_0) = (1 - z, \text{const} - z, \mathbf{0})$ . Sovran *et al.* [13] studied the linear stability of this solution. They analytically found the critical Rayleigh number beyond which this solution loses its stability. They showed that, for  $\psi \geq \psi_{\text{mono}}$ , where  $\psi_{\text{mono}} = 1/[(40/51)Le - 1]$ , this solution loses its stability via a stationary bifurcation leading to a monocellular flow and the corresponding critical Rayleigh number is  $Ra_{cs} = 12/(Le\psi)$ .

## III. ANALYTICAL SOLUTION OF THE MONOCELLULAR FLOW

In the limit of a shallow cavity  $A \gg 1$ , we use the parallel flow approximation used by Ouriemi *et al.* [14]. The basic flow, denoted by a subscript 0, is then given as follows:

$$\mathbf{V}_0 = U_0(z) \hat{\mathbf{e}}_x; \quad T_0 = bx + f(z); \quad C_0 = mx + g(z). \quad (5)$$

For the stationary state, by using the above mentioned assumptions and the corresponding boundary conditions, we obtain the velocity, temperature and concentration fields

$$\begin{aligned} T_0 &= 1 - z, \\ U_0 &= Ra m \psi / (1/2 - z), \\ C_0 &= mx + [m^2 Ra Le \psi (3z^2 - 2z^3)] / (12 - z \\ &\quad - (m^2 Ra Le \psi) / 24 + (1 - mA) / 2, \\ m &= \pm \sqrt{(10 Le Ra \psi - 120) / (Le Ra \psi)}. \end{aligned} \quad (6)$$

Three remarks can be made concerning the expression of the parameter  $m$  in the concentration field. (a) The expres-

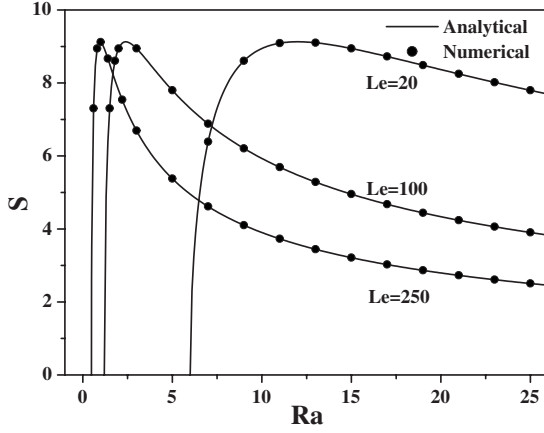


FIG. 1. Separation curve for  $Le=20, 100, 250, \psi=0.1, \varepsilon^*=0.5$ .

sion under the square root must be positive, which means that  $Ra > 12/(Le \psi)$ ; this value of  $Ra$  corresponds to the critical Rayleigh number of the onset of convection [13]. (b)  $m$  is negative or positive according to whether the flow is clockwise or anticlockwise and both solutions are possible depending on the initial conditions. (c) Separation is defined as the difference of the mass fractions of the denser species between the two ends, left and right, of the cell  $S = mA$ , so we can easily find that the maximum separation is obtained for  $Ra = 24/(Le \psi)$ . This value will be denoted as  $Ra_{opt}$ .

Figure 1 presents the variation of separation with Rayleigh number  $Ra$ . It can be seen that the separation has a maximum; this maximum corresponds to the optimal coupling between thermodiffusion and convection. If  $Ra$  is small, the convection is weak and separation is mainly due to thermodiffusion and in this case it is small. If  $Ra$  is large, the convection is intense and the flow remixes the species of the mixture and we obtain a small separation. It will be noted that due to the reference scale used for the concentration field, the separation  $S$  may be higher than 1.

#### IV. LINEAR STABILITY ANALYSIS OF THE MONOCELLULAR FLOW

In order to study the stability of the monocellular solution, it is convenient to rewrite the governing equations using the perturbations of velocity  $\mathbf{v}$ , temperature  $\theta$ , pressure  $p$ , and concentration  $c$ :

$$\mathbf{v} = \mathbf{V} - \mathbf{V}_0, \quad \theta = T - T_0, \quad c = C - C_0, \quad p = P - P_0.$$

By neglecting second order terms, we obtain the linear equations where the unknowns are the disturbances.

To take the boundary conditions for the temperature and the concentration at  $z=0,1$  into account more easily, we introduce the new variable  $\eta = c - \theta$ . By developing the disturbances in normal modes  $(w, \theta, \eta) = [w(z), \theta(z), \eta(z)]e^{(ikx + \sigma t)}$ , we obtain the following system of equations:

$$(D^2 - k^2)w = -Ra k^2[\theta(1 + \psi) + \psi\eta],$$

$$\sigma\theta - w + Ik\theta U_0 = (D^2 - k^2)\theta,$$

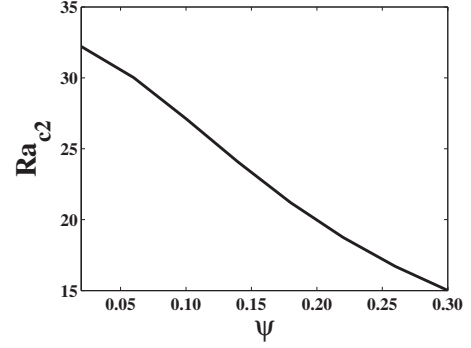


FIG. 2. Critical Rayleigh number  $Ra_{c2}$  for the bifurcation from the monocellular flow to the multicellular flow, function of the separation ratio  $\psi$ , for  $Le=100, \varepsilon^*=0.5$ .

$$\begin{aligned} \varepsilon\sigma Ik(\eta + \theta) - k^2 U_0(\eta + \theta) - mDw + Ik w D C_0 \\ = (1/Le)Ik(D^2 - k^2)\eta, \end{aligned} \quad (7)$$

where  $D = \partial/\partial z$ ,  $k$  is the horizontal wave number,  $\sigma = \sigma_r + I\sigma_i$  is the temporal amplification of the perturbation, and  $I^2 = -1$ .

The corresponding boundary conditions are

$$w = 0, \quad \theta = 0, \quad \frac{\partial \eta}{\partial z} = 0 \quad \text{at } z = 0, 1. \quad (8)$$

The resulting linear problem is solved by means of a fifth order Galerkin method, using the following expansions:

$$\begin{aligned} w = \sum_{i=1}^N a_i(z-1)z^i, \quad \theta = \sum_{i=1}^N b_i(z-1)z^i, \\ \eta = c_1 + c_2(z^2 - 2z^3/3) + \sum_{i=1}^{N-2} c_{i+2}(z-1)^2 z^{i+1}. \end{aligned}$$

Critical values of the Rayleigh number were obtained for stationary and nonstationary bifurcations. For the values of  $\psi$  and  $Le$  studied, the critical Rayleigh number leading to stationary bifurcation is always greater than that leading to Hopf bifurcation. So, in this study, we mainly present the values of the critical wave number  $k_{c2}$ , the critical Rayleigh number  $Ra_{c2}$ , and the critical frequency  $\omega_{c2}$  associated with the Hopf bifurcation. The stability diagrams  $Ra_{c2} = f(\psi)$ ,  $k_{c2} = f(\psi)$ , and  $\omega_{c2} = f(\psi)$  are illustrated in Figs. 2–4 for  $Le = 100$  and  $\varepsilon^* = 0.5$ . For a layer heated from below we note that  $Ra_{c2}$  decreases with the separation ratio, which means that the thermodiffusion destabilizes the monocellular flow. The critical frequency always increases with  $\psi$ . The stability study has enabled us to define the interval of variation of  $Ra$  where the monocellular flow remains stable thus making it possible to separate the species of the mixture.

#### V. NUMERICAL SIMULATIONS

The equation system (3) with the associated boundary conditions (4) was solved numerically using a collocation

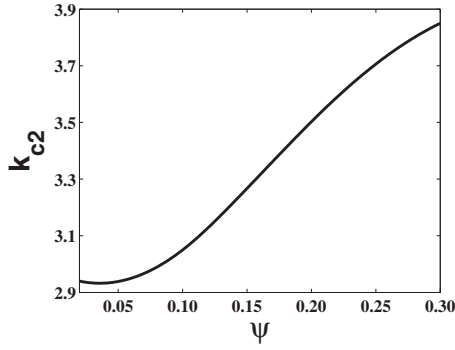


FIG. 3. Critical wave number  $k_{c2}$  for the bifurcation from the monocellular flow to the multicellular flow, function of the separation ratio  $\psi$  for  $Le=100$ ,  $\varepsilon^*=0.5$ .

spectral method [15], well known for its accuracy and a finite element method (Comsol industrial code) with a rectangular grid system, better suited to the rectangular shape of the cell used. For the spectral method, the time scheme was a second order Adams-Bashforth-Euler backward scheme. For the collocation method, the spatial resolution was  $100 \times 20$  collocation points along the horizontal and vertical axes, respectively, and for Comsol the spatial resolution was  $150 \times 30$ .

We found a good agreement between the analytical and the numerical results, obtained by the two methods, concerning the separation for  $Le=(20,100,250)$ ,  $\varepsilon^*=0.5$ ,  $A=20$  and for different values of  $\psi$ . In Fig. 1 we present the results for the case  $\psi=0.1$ .

For  $Le=(20,100,250)$ ,  $\psi=0.1$ ,  $\varepsilon^*=0.5$ , Fig. 5 shows the isoconcentrations and streamlines for the corresponding optimal Rayleigh number ( $Ra_{opt}=12$  for  $Le=20$ ,  $Ra_{opt}=2.4$  for  $Le=100$ , and  $Ra_{opt}=0.96$  for  $Le=250$ ) and Fig. 6 shows the isoconcentrations and streamlines for  $Ra=25$ . A monocellular flow is observed in these cases. Due to thermodiffusion, the denser species of the mixture moves towards the top cold wall while the other moves towards the bottom hot wall ( $\psi > 0$ ), the monocellular flow advects one of the species of the mixture towards the right part of the cavity and the other one towards the left part. This results in a high concentration of one species in the left part of the cell and a high concentration of the other species in the right part, leading to a hori-

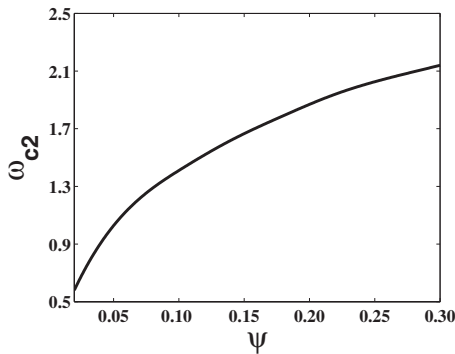


FIG. 4. Critical pulsation  $\omega_{c2}$  for the bifurcation from the monocellular flow to the multicellular flow, function of the separation ratio  $\psi$  for  $Le=100$ ,  $\varepsilon^*=0.5$ .

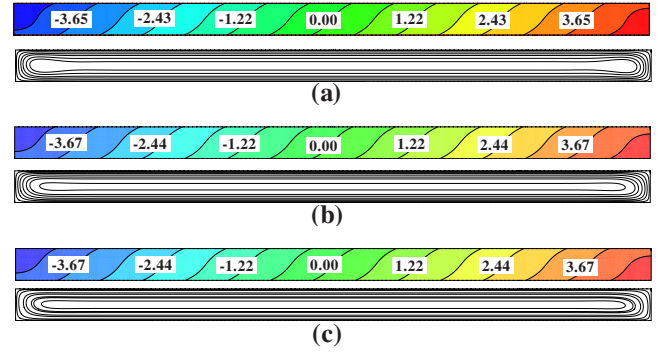


FIG. 5. (Color online) Isoconcentrations and streamlines for the optimal Rayleigh numbers for  $\psi=0.1$ ,  $\varepsilon^*=0.5$  and for (a)  $Le=20$ ,  $Ra=12$ , (b)  $Le=100$ ,  $Ra=2.4$ , and (c)  $Le=250$ ,  $Ra=0.96$ .

zontal stratification of the concentration field and a separation of the species of the mixture.

The results of the linear stability study give  $Ra_{c2}=32.64$ ,  $k_{c2}=2.80$ , and  $\omega_{c2}=2.30$  for  $Le=20$ ,  $\psi=0.1$ , and  $\varepsilon^*=0.5$  in an infinite cell. Using an aspect ratio  $A=10$  in the numerical study, we observe that the flow remains quasimonocellular while all the physical fields ( $V, T, C, P$ ) oscillate. The oscillations appear just before  $Ra_{c2}=32.64$  but they disappear rapidly, whereas for  $(Ra=33.5, \omega=2.36)$ ,  $(Ra=34, \omega=2.14)$ ,  $(Ra=34.5, \omega=2.20)$  the quasimonocellular flow remains oscillatory for a long time. For  $Ra=35.7$  we obtain a flow with nine convective cells corresponding to  $k_{cnum}=2.827$  [ $k_{cnum}=(n\pi)/A$  where  $n$  is the number of convective cells]. For  $Le=100$  and  $\psi=0.1$ , we obtain  $Ra_{c2}=27.48$ ,  $k_{c2}=3.08$ , and  $\omega_{c2}=1.44$  by the linear stability analysis. By the direct numerical simulation we find that the oscillations begin at  $Ra=27$ ; for this value of  $Ra$  the oscillations appear for a very short time, whereas for  $(Ra=28, \omega=1.4)$ ,  $(Ra=29, \omega=1.43)$ ,  $(Ra=30, \omega=1.42)$ ,  $(Ra=31, \omega=1.4)$ , and  $(Ra=32, \omega=1.33)$ , the oscillations remain for a very long time. Figure 7 shows a typical instantaneous streamline pattern for  $Le=100$ ,  $Ra=28$  during the oscillation. We observe that we have many convective cells. To find the corresponding wave number we calculate the distance  $x$  between the centers of two adjacent convective cells. We estimate  $x$  to be 2.07, so the corre-

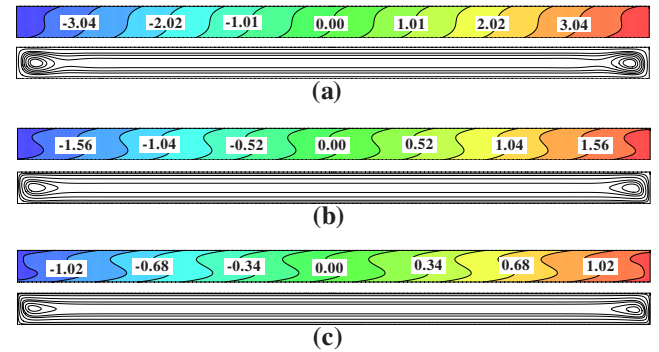


FIG. 6. (Color online) Isoconcentrations and streamlines for  $\psi=0.1$ ,  $\varepsilon^*=0.5$ ,  $Ra=25$  and for (a)  $Le=20$ , (b)  $Le=100$ , and (c)  $Le=250$ .



FIG. 7. A typical instantaneous streamline pattern for  $Le=100$ ,  $\psi=0.1$ ,  $Ra=28$  during the oscillation.

sponding wave number is  $kc_{\text{num}}=(2\pi)/x=3.03$  which is in good agreement with the wave number obtained from the linear stability analysis. The difference between the values obtained numerically and those obtained by the Galerkin method may be due either to the hypothesis made for the determination of the analytical solution, or to the aspect ratio used in the numerical simulation, because the linear stability was developed for an infinite cell.

## VI. SEPARATION RESULTS OBTAINED IN A THERMOGRAVITATIONAL COLUMN AND IN RAYLEIGH-BENARD CONFIGURATION

To show the practical interest of the horizontal configuration of the thermogravitational cell, we compare it to the vertical configuration. We studied thermogravitation in a vertical cell of height  $H$  and thickness  $e$ . The vertical walls of the cavity were maintained at constant and different temperatures. The equations governing this problem are given in Eq. (3) and the corresponding boundary conditions are

$$\begin{aligned} T &= 0 \quad \text{for } x=0, \quad T = 1 \quad \text{for } x=1, \\ \nabla C \cdot \mathbf{n} &= \nabla T \cdot \mathbf{n} \quad \text{for } x=0,1, \\ \partial T / \partial z &= \partial C / \partial z = 0 \quad \text{for } z=0,A, \\ \mathbf{V} \cdot \mathbf{n} &= 0, \quad \forall M \in \partial\Omega. \end{aligned} \quad (9)$$

We use the same assumptions used in the case of a horizontal cell. To obtain a simple expression for the fields, we neglect the term  $\psi C$  in the momentum transport equation; it has been shown that this assumption is valid for most of the mixtures considered.

By solving the equations with the corresponding boundary conditions and the above-mentioned assumptions, we obtain the following expressions for velocity, temperature, and concentration fields:

$$\begin{aligned} T_0 &= x, \\ W_0 &= Ra(x - 1/2), \\ C_0 &= mz + m Ra Le(x^3/6 - x^2/4) + x, \\ &+ (m Ra Le)/24 - 1/2 - (mA)/2, \\ m &= (10 Le Ra)/(Le^2 Ra^2 + 120). \end{aligned} \quad (10)$$

In this case the separation is defined by  $S=mA$ , where  $A=H/e$ . By observing the expression of  $m$  we note that there is a maximum separation for  $Ra=\sqrt{120/Le}$ . This value will be denoted as  $Ra_{\text{optv}}$ .

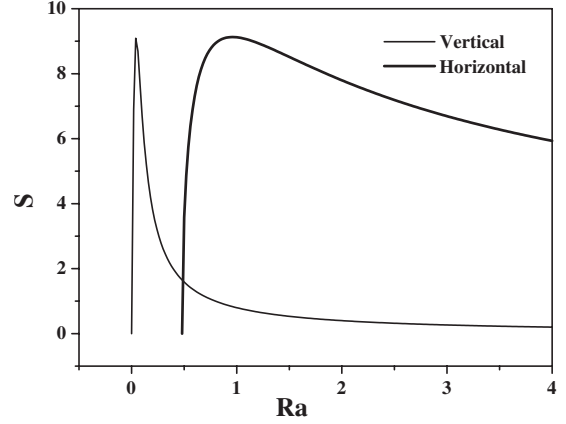


FIG. 8. Separation in horizontal and vertical cells for  $Le=250$ ,  $\psi=0.1$ ,  $\epsilon^*=0.5$ .

By replacing the optimal values of  $Ra$  in the expressions of vertical and horizontal separation we obtain the same maximum separation values for both configurations  $S_{v \text{ max}} = (\sqrt{30}/12)A = S_{h \text{ max}}$ . Thus the maximum separations in the vertical and horizontal cases are equal. To show the advantage of the horizontal configuration, we will compare the values of the optimal Rayleigh number in the horizontal and vertical cases  $r = Ra_{\text{opt}}/Ra_{\text{optv}} = (\Delta T_h/\Delta T_v)(H/e) \approx 2.2/\psi$ , where  $\Delta T_h$  is the temperature difference between the horizontal walls of the horizontal cell,  $\Delta T_v$  the temperature difference between the two vertical walls of the vertical cell,  $H$  the height of the horizontal cell, and  $e$  the width of the vertical cell. For example, if we consider the binary mixture used by Platten *et al.* [5] (water ethanol mixture 60.88 wt % water), we obtain  $\psi \approx 0.2$ , and thus  $r \approx 11$ . The major disadvantage of the vertical cell was always the narrow width of the cavity ( $\approx 0.2$  mm) required to obtain high separation [2]. By using a horizontal cell, we obtain the same maximum separation with a height 11 times larger than the width of the vertical column for the same difference of temperature, which is easier to realize in experiments and which allows us to obtain a greater quantity of species. Another disadvantage of the vertical cell is the fast decrease of separation when the Rayleigh number increases from the optimal value. On the other hand, in the case of the horizontal cell we notice a slow decrease of separation when the Rayleigh number increases (Fig. 8); a Rayleigh number higher than the optimal Rayleigh number can therefore be used without significant loss of the level of separation.

## VII. CONCLUSIONS

We have proposed a configuration for the separation of the components of a binary fluid mixture in a porous medium using thermogravitation. We have studied the monocellular flow appearing at the onset of convection in a binary fluid saturating a horizontal porous cavity heated from below. If the separation ratio  $\psi$  is positive and greater than a certain value  $\psi_{\text{mono}}$ , it has been shown that it is possible to separate the species of the binary fluid mixture between the two ends of the cell. The monocellular flow obtained after the loss of

stability of the rest solution, and which allows separation, remains stable beyond the Rayleigh number corresponding to the optimal separation (i.e.,  $Ra_{c2} > Ra_{opt}$ ). Moreover, the optimal Rayleigh number in the horizontal cell is larger than that of the vertical one, which permits us to perform separation in the cell of greater height. In addition, numerical simu-

lations have been carried out with a spectral method and a finite element method. In all the cases studied, good agreement has been found between the analytical results and the numerical ones for both the separation and the critical values of the transition between the monocellular flow and the multicellular one.

- 
- [1] K. Clusius and G. Dickel, *Naturwiss.* **6**, p. 546 (1938).  
 [2] W. H. Furry, R. C. Jones, and L. Onsager, *Phys. Rev.* **55**, 1083 (1939).  
 [3] S. R. De Groot, *Physica (Amsterdam)* **8**, 801 (1942).  
 [4] M. Lorenz and A. H. Emery, *Chem. Eng. Sci.* **11**, 16 (1959).  
 [5] J. K. Platten, M. M. Bou-Ali, and J. F. Dutrieux, *J. Phys. Chem. B* **107**, 11763 (2003).  
 [6] G. Labrosse, *Phys. Fluids* **15**, 2694 (2003).  
 [7] I. I. Ryzhkov and V. M. Shevtsova, *Phys. Fluids* **19**, 027101 (2007).  
 [8] M. M. Bou-Ali, O. Ecenarro, J. A. Madariaga, C. M. Santamaría, and J. J. Valencia, *Phys. Rev. E* **59**, 1250 (1999).  
 [9] M. M. Bou-Ali, O. Ecenarro, J. A. Madariaga, C. M. Santamaría, and J. J. Valencia, *Phys. Rev. E* **62**, 1420 (2000).  
 [10] B. Elhajjar, A. Mojtabi, M. Marcoux, and M. C. Charrier-Mojtabi, *C. R. Mec.* **334**, 621 (2006).  
 [11] E. Knobloch, *Phys. Rev. A* **34**, 1538 (1986).  
 [12] J. K. Platten and J. C. Legros, *Convection in Liquids* (Springer-Verlag, Berlin, 1984), p. 595.  
 [13] O. Sovran, M. C. Charrier-Mojtabi, and A. Mojtabi, *C. R. Acad. Sci., Ser. Iib Mec.* **4**, 287 (2001).  
 [14] M. Ouriemi, P. Vasseur, A. Bahloul, and L. Robillard, *Int. J. Therm. Sci.* **45**, 752 (2006).  
 [15] M. Azaiez, C. Bernardi, and M. Grundmann, *Numer. Math.* **2**, 91 (1994).